GEM CEDAR modeling challenge: Ionospheric conductivity

State of ionospheric conductivity research and what's coming next (or should)

CCAR

Outline

Fundamentals:

What is conductivity and what is needed to calculate it?

Current understanding/modeling:

What is the current state of understanding based on our previous modeling?

What's next:

One new approach and significance

Outline

Fundamentals:

What is conductivity and what is needed to calculate it?

Current understanding/modeling:

What is the current state of understanding based on our previous modeling?

What's next:

A new app

Conclusions:

Different approaches = different pictures

Consistent picture dependent on bringing together diverse data

Creating a capable model that can be implemented in MI models is the goal

Ionospheric Conductivity

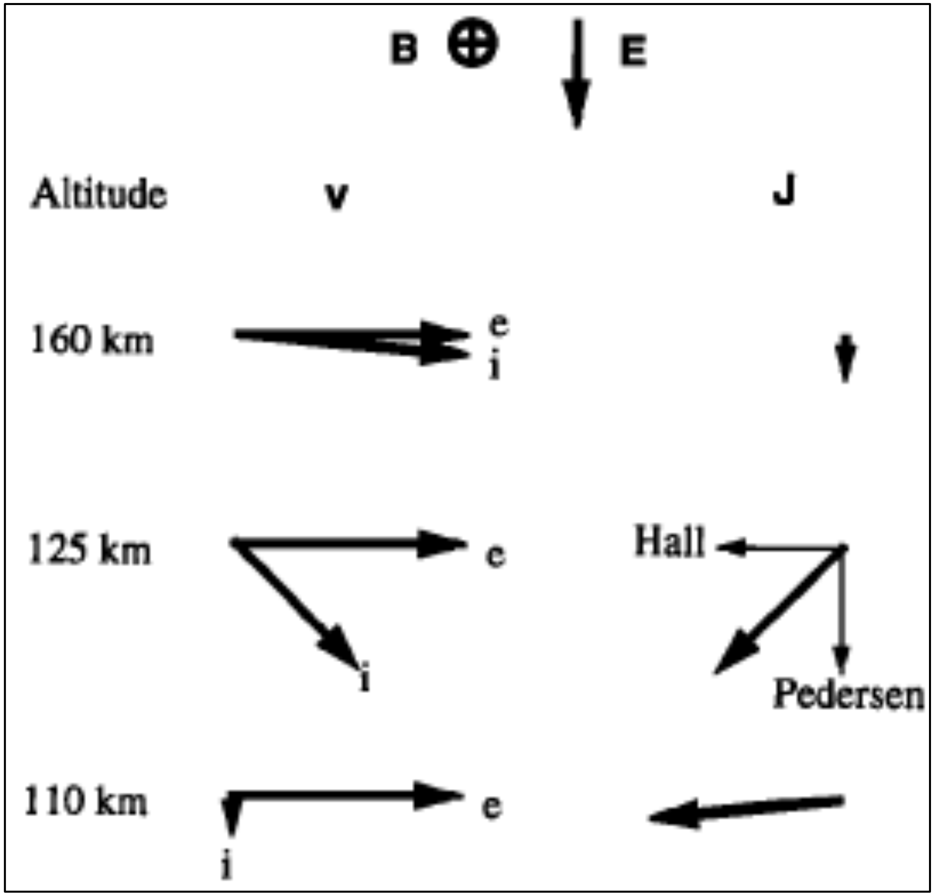

Richmond and Thayer [2013]

$$\mathbf{J} = \tilde{\sigma} \cdot \mathbf{E}$$

$$= \sigma_P \mathbf{E}_\perp + \sigma_H \hat{\mathbf{B}} \times \mathbf{E} + \sigma_\| \mathbf{E}_\|$$

$$\tilde{\sigma} = \begin{bmatrix} \sigma_P & -\sigma_H & 0 \\ \sigma_H & \sigma_P & 0 \\ 0 & 0 & \sigma_\| \end{bmatrix}$$

$$\int_h \sigma_x \mathrm{d}h = \Sigma_x$$

Ionospheric Conductivity

Typical profiles

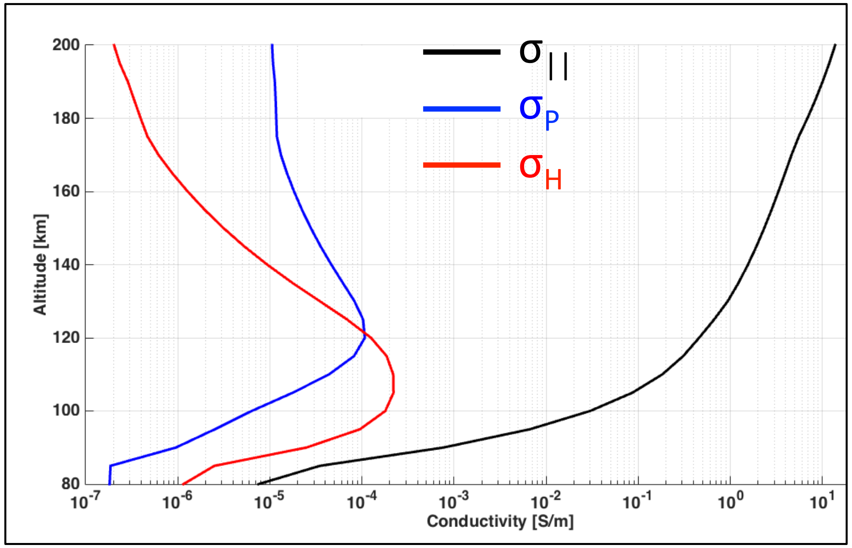

$$\mathbf{J} = \tilde{\sigma} \cdot \mathbf{E}$$

$$= \sigma_P \mathbf{E}_\perp + \sigma_H \hat{\mathbf{B}} \times \mathbf{E} + \sigma_\parallel \mathbf{E}_\parallel$$

$$\tilde{\sigma} = \begin{bmatrix} \sigma_P & -\sigma_H & 0 \\ \sigma_H & \sigma_P & 0 \\ 0 & 0 & \sigma_\parallel \end{bmatrix}$$

$$\int_h \sigma_x \mathrm{d}h = \Sigma_x$$

Ionospheric Conductivity

$$\tilde{\sigma} = \begin{bmatrix} \sigma_P & -\sigma_H & 0 \\ \sigma_H & \sigma_P & 0 \\ 0 & 0 & \sigma_{||} \end{bmatrix}$$

$$\sigma_{||} = \frac{n_e e^2}{m_e \left(\sum_i \nu_{ei} + \sum_n \nu_{en} \right)}$$

$$\sigma_H = -\sum_i \left(\frac{n_i e_i^2}{m_i \nu_{in}} \right) \frac{\nu_{in} \omega_{c_i}}{\nu_{in}^2 + \omega_{c_i}^2} + \left(\frac{n_e e^2}{m_e \nu_{en}} \right) \frac{\nu_{en} \omega_{c_e}}{\nu_{en}^2 + \omega_{c_e}^2}$$

$$\sigma_P = \sum_i \left(\frac{n_i e_i^2}{m_i \nu_{in}} \right) \frac{\nu_{in}^2}{\nu_{in}^2 + \omega_{c_i}^2} + \left(\frac{n_e e^2}{m_e \nu_{en}} \right) \frac{\nu_{en}^2}{\nu_{en}^2 + \omega_{c_e}^2}$$

The equations are often written in different forms

Ionospheric Conductivity

$$\tilde{\sigma} = \begin{bmatrix} \sigma_P & -\sigma_H & 0 \\ \sigma_H & \sigma_P & 0 \\ 0 & 0 & \sigma_{||} \end{bmatrix}$$

$$\sigma_{||} = \frac{n_e e^2}{m_e \left(\sum_i \nu_{ei} + \sum_n \nu_{en} \right)}$$

$$\nu_{x_1 x_2} = x_1 \rightarrow x_2 \text{ collision frequency}$$

$$\sigma_H = -\sum_i \left(\frac{n_i e_i^2}{m_i \nu_{in}} \right) \frac{\nu_{in}\omega_{ci}}{\nu_{in}^2 + \omega_{ci}^2} + \left(\frac{n_e e^2}{m_e \nu_{en}} \right) \frac{\nu_{en}\omega_{ce}}{\nu_{en}^2 + \omega_{ce}^2}$$

$$\omega_c = \frac{|e|B}{m}$$

$$\sigma_P = \sum_i \left(\frac{n_i e_i^2}{m_i \nu_{in}} \right) \frac{\nu_{in}^2}{\nu_{in}^2 + \omega_{ci}^2} + \left(\frac{n_e e^2}{m_e \nu_{en}} \right) \frac{\nu_{en}^2}{\nu_{en}^2 + \omega_{ce}^2}$$

The equations are often written in different forms

What is needed to calculate conductivity?

Magnetic field

Neutral composition

Temperature

Ion/electron densities

What is needed to calculate conductivity?

To get these we need

Magnetic field Neutral composition Temperature Ion/electron densities	Ion production rates From solar photons and precipitating particles Collisions Plasma drift Equilibrium densities

Ion production: Two contributions

Solar photons

Magnetospheric particles

Solar Contribution

Fundamentals - **Current Understanding/Modeling** - What's next?

Brekke and Moen [1993]

Author	Year	Σ_P	Σ_H
Schuster	1889, 1908	$a+b\cdot\cos\chi$	
Appleton	1937	$\text{const.}\cdot(\cos\chi)^{3/2}$ $(\nu \gg \omega)$	
Metha	1978	$7.1\cdot(\cos\chi)^{0.44}$	$13.7(\cos\chi)^{0.45}$
Senior	1980	$9.6\cdot\cos\chi+1.6$	$15.8\cdot\cos\chi+2.3$
Vickrey *et al.*	1981	$5\cdot(\cos\chi)^{1/2}$	$10\cdot(\cos\chi)^{1/2}$
de la Beaujardière *et al.*	1982	$10\cdot\cos\chi+2$	$16\cdot\cos\chi+3$
Robinson and Vondrak*	1984	$0.88\sqrt{S_a}(\cos\chi)^{1/2}$	$1.5\sqrt{S_a}(\cos\chi)^{1/2}$
Rasmussen *et al.*†	1988	$(4.5/\mathbf{B})(1-0.85\cdot v^2)\cdot(1+0.15u+0.05u^2)$	$(5.6/\mathbf{B})\cdot(1-0.9v^2)\cdot(1+0.15u+0.005u^2)$
Schlegel	1988	$6.4\cdot(\cos(\chi-12^\circ))^{0.54}$	
Brekke and Hall	1988	$3.05\cos\chi+4.06(\cos\chi)^{1/2}$	$6.24\cos\chi+2.85(\cos\chi)^{1/2}$
Senior	1991	$1.81+8.88\cos\chi$	$21.58-0.21\cdot\chi$
Moen and Brekke	1992	$S_a^{0.49}\cdot(0.34\cos\chi+0.93\cdot(\cos\chi)^{1/2})$	$S_a^{0.53}(0.81\cos\chi+0.54(\cos\chi)^{1/2})$

* S_a being the daily 10.7 cm solar radio flux at Ottawa in units of $10^{-22}\,\mathrm{W\,m^{-2}\,Hz^{-1}}$ (adjusted to 1 A.U.).
† v is the normalized zenith angle, $v=\chi/90^\circ$, u is the normalized solar flux, $u=S_a/90$. **B** is the magnetic field strength.

Richmond and Kamide [1998]

$$\Sigma_H(\chi,\mathrm{F}_{10.7}) = \begin{cases} 1.8\mathrm{F}_{10.7}^{1/2}\cos(\chi) & \text{for } \chi \le 65, \\ \Sigma_H(65,\mathrm{F}_{10.7}) - 0.27(\chi-65) & \text{for } \chi > 65, \end{cases}$$

$$\Sigma_P(\chi,\mathrm{F}_{10.7}) = \begin{cases} 0.5\mathrm{F}_{10.7}^{2/3}\cos(\chi)^{2/3} & \text{for } \chi \le 65, \\ \Sigma_P(65,\mathrm{F}_{10.7}) - 0.22(\chi-65) & \text{for } 65 < \chi \le 100, \\ \Sigma_P(100,\mathrm{F}_{10.7}) - 0.13(\chi-100) & \text{for } \chi > 100, \end{cases}$$

Used in AMIE procedure

Solar Contribution

Brekke and Moen [1993]

Author	Year	Σ_P	Σ_H
Schuster	1889, 1908	$a+b\cdot\cos\chi$	
Appleton	1937	$\text{const.}\cdot(\cos\chi)^{3/2}\ (\nu \gg \omega)$	
Metha	1978	$7.1\cdot(\cos\chi)^{0.44}$	$13.7(\cos\chi)^{0.45}$
Senior	1980	$9.6\cdot\cos\chi+1.6$	$15.8\cdot\cos\chi+2.3$
Vickrey *et al.*	1981	$5\cdot(\cos\chi)^{1/2}$	$10\cdot(\cos\chi)^{1/2}$
de la Beaujardière *et al.*	1982	$10\cdot\cos\chi+2$	$16\cdot\cos\chi+3$
Robinson and Vondrak*	1984	$0.88\sqrt{S_a}(\cos\chi)^{1/2}$	$1.5\sqrt{S_a}(\cos\chi)^{1/2}$
Rasmussen *et al.*†	1988	$(4.5/\mathbf{B})(1-0.85\cdot v^2)\cdot(1+0.15u+0.05u^2)$	$(5.6/\mathbf{B})\cdot(1-0.9v^2)\cdot(1+0.15u+0.005u^2)$
Schlegel	1988	$6.4\cdot(\cos(\chi-12^\circ))^{0.54}$	
Brekke and Hall	1988	$3.05\cos\chi+4.06(\cos\chi)^{1/2}$	$6.24\cos\chi+2.85(\cos\chi)^{1/2}$
Senior	1991	$1.81+8.88\cos\chi$	$21.58-0.21\cdot\chi$
Moen and Brekke	1992	$S_a^{0.49}\cdot(0.34\cos\chi+0.93\cdot(\cos\chi)^{1/2})$	$S_a^{0.53}(0.81\cos\chi+0.54(\cos\chi)^{1/2})$

* S_a being the daily 10.7 cm solar radio flux at Ottawa in units of $10^{-22}\,\mathrm{W\,m^{-2}\,Hz^{-1}}$ (adjusted to 1 A.U.).
† v is the normalized zenith angle, $v=\chi/90^\circ$, u is the normalized solar flux, $u=S_a/90$. **B** is the magnetic field strength.

Richmond and Kamide [1988]

$$\Sigma_H(\chi,\mathrm{F}_{10.7}) = \begin{cases} 1.8\mathrm{F}_{10.7}^{1/2}\cos(\chi) & \text{for } \chi \le 65, \\ \Sigma_H(65,\mathrm{F}_{10.7}) - 0.27(\chi-65) & \text{for } \chi > 65, \end{cases}$$

$$\Sigma_P(\chi,\mathrm{F}_{10.7}) = \begin{cases} 0.5\mathrm{F}_{10.7}^{2/3}\cos(\chi)^{2/3} & \text{for } \chi \le 65, \\ \Sigma_P(65,\mathrm{F}_{10.7}) - 0.22(\chi-65) & \text{for } 65 < \chi \le 100, \\ \Sigma_P(100,\mathrm{F}_{10.7}) - 0.13(\chi-100) & \text{for } \chi > 100, \end{cases}$$

Used in AMIE procedure

Additional considerations?

Ridley et al., [2004]

Auroral Contribution

Much more uncertain component

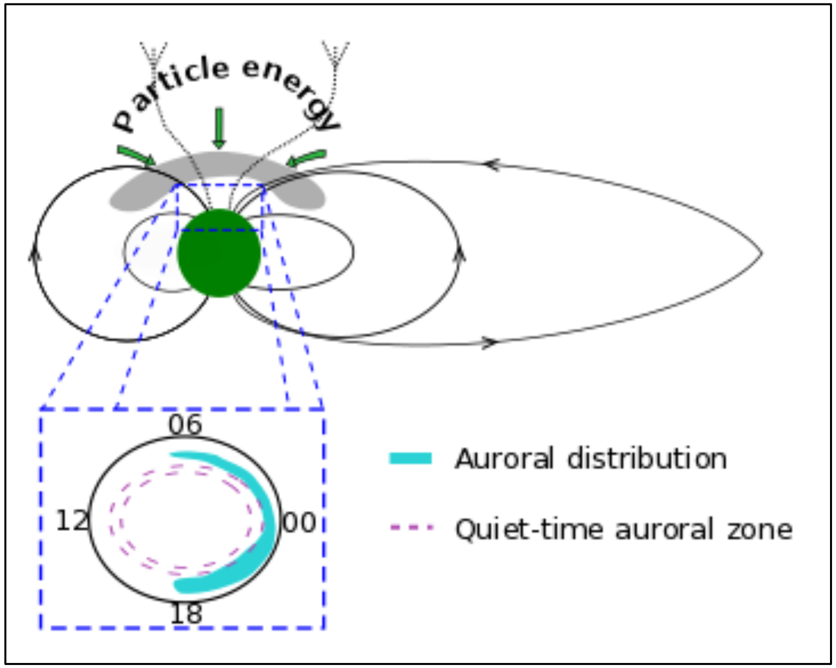

Auroral Contribution

Many approaches:

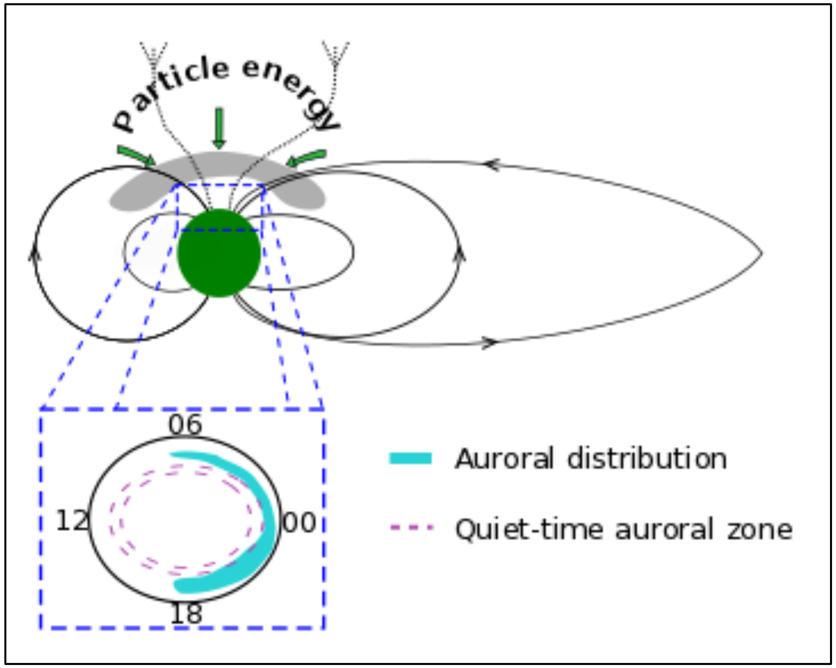

- Particle data
- Emission data
- Magnetometer data
  - Ground-based
  - Indirect space-based
- Multiple data sources at once

Auroral Contribution

Precipitation characteristics → [black box] → **Conductances**

Auroral Contribution

Fundamentals - **Current Understanding/Modeling** - What's next?

Auroral Contribution

Fundamentals - **Current Understanding/Modeling** - What's next?

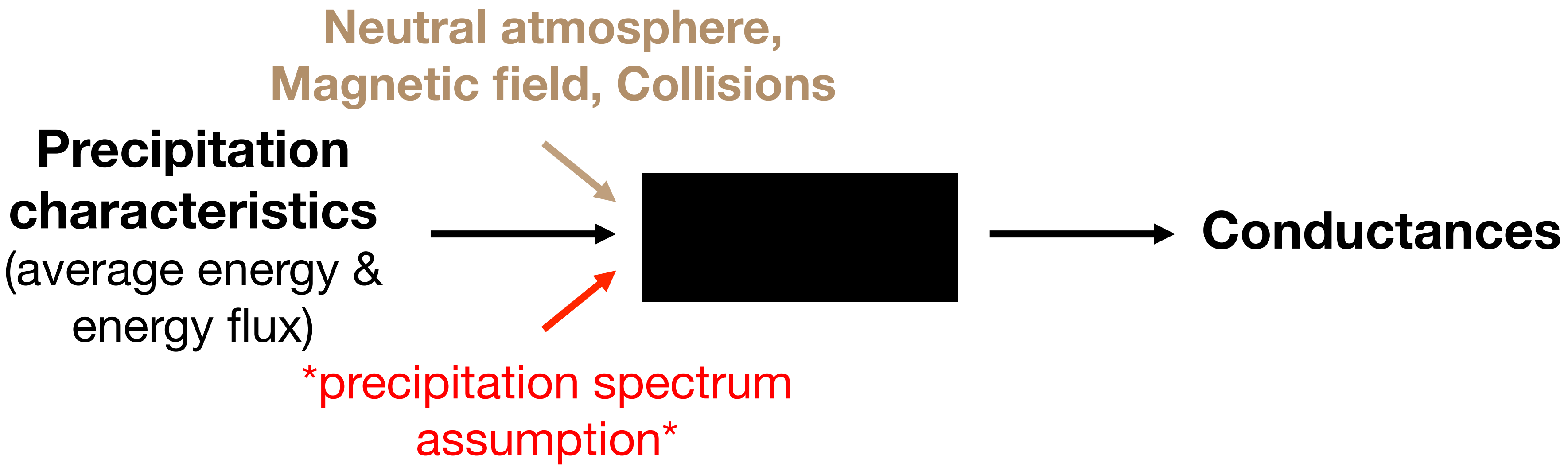

1. Relationships between precipitating particles and conductances

Electrons

Spiro et al., [1982]

Robinson et al., [1987]

Protons

Hardy et al., [1989]

2. Models of conductance due to precipitating particles

Electrons

Hardy et al., [1987]

Fuller-Rowell and Evans, [1987]

Protons

Galand and Richmond, [2001]

Maxwellian energy particle precipitation assumption

and

Robinson formulas

$$\Sigma_P = \frac{40E}{16 + E^2}\,\Phi_E^{\,1/2}$$

$$\frac{\Sigma_H}{\Sigma_P} = 0.45(E)^{0.85}$$

Robinson et al., [1987]

Electrons → Conductance

Fundamentals - **Current Understanding/Modeling** - What's next?

Height-integrated Pedersen conductances inferred from DMSP particle precipitation observations

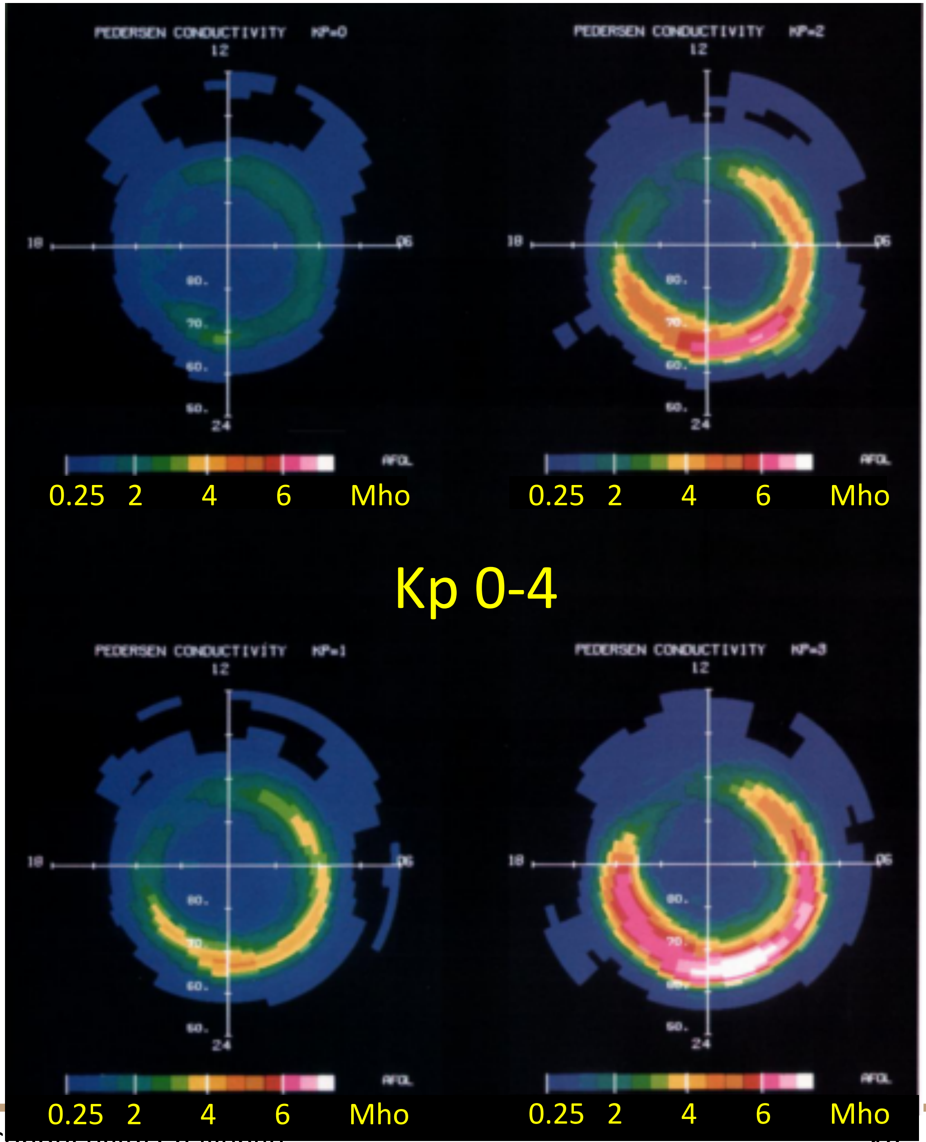

Maxwellian precipitation assumption

Hardy et al., [1987]

Electrons ➔ Conductance

Fundamentals - **Current Understanding/Modeling** - What's next?

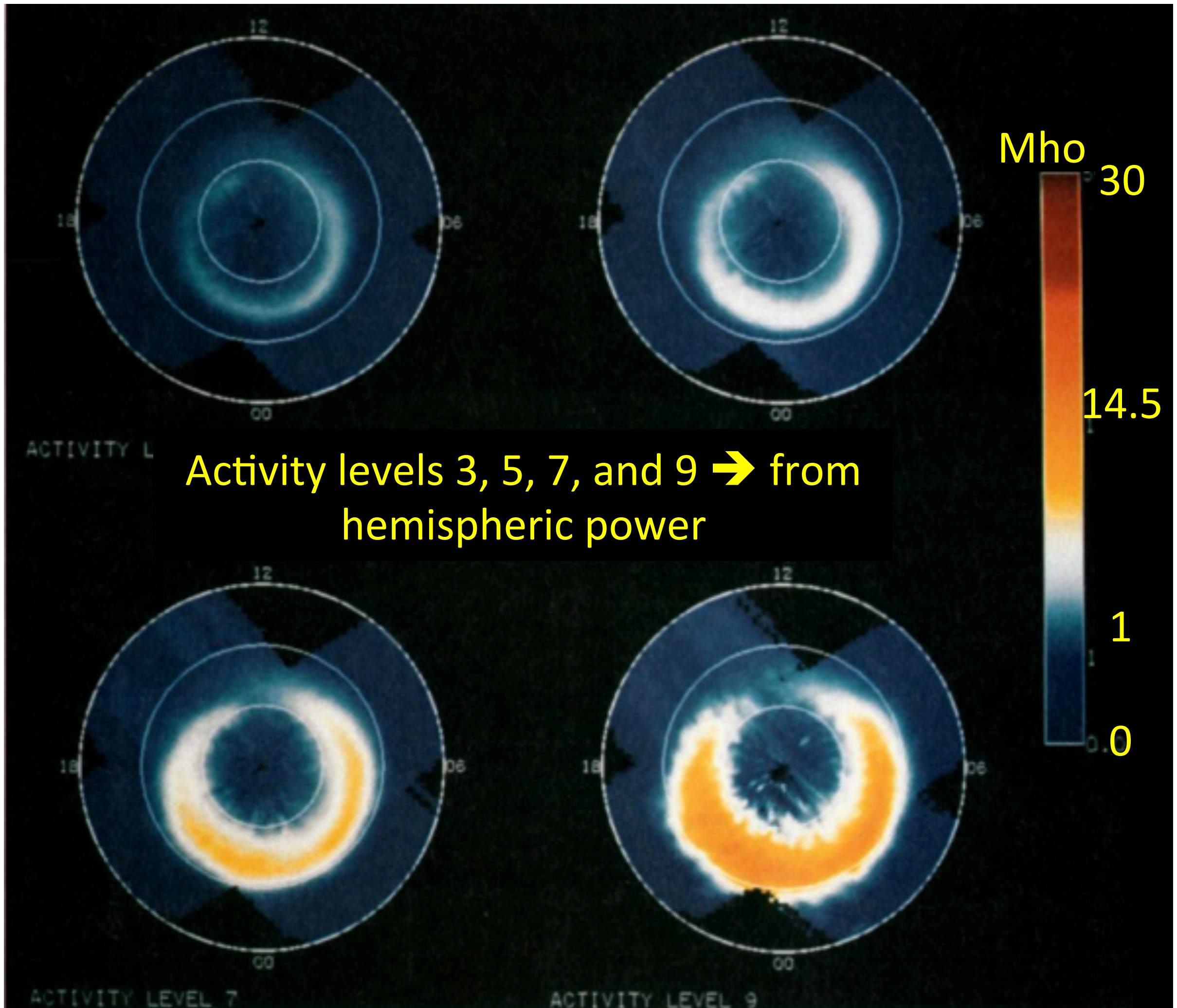

Height-integrated Pedersen conductances inferred from TIROS/NOAA particle precipitation observations

Functional spectral precipitation assumption

Fuller-Rowell and Evans, [1987]

Emission data

Neutral atmosphere, Magnetic field, Collisions

Auroral emissions → **Precipitation characteristics** (average energy & energy flux) → → **Conductances**

precipitation spectrum assumption

Emission data

GUVI auroral images used to create Kp-based auroral model

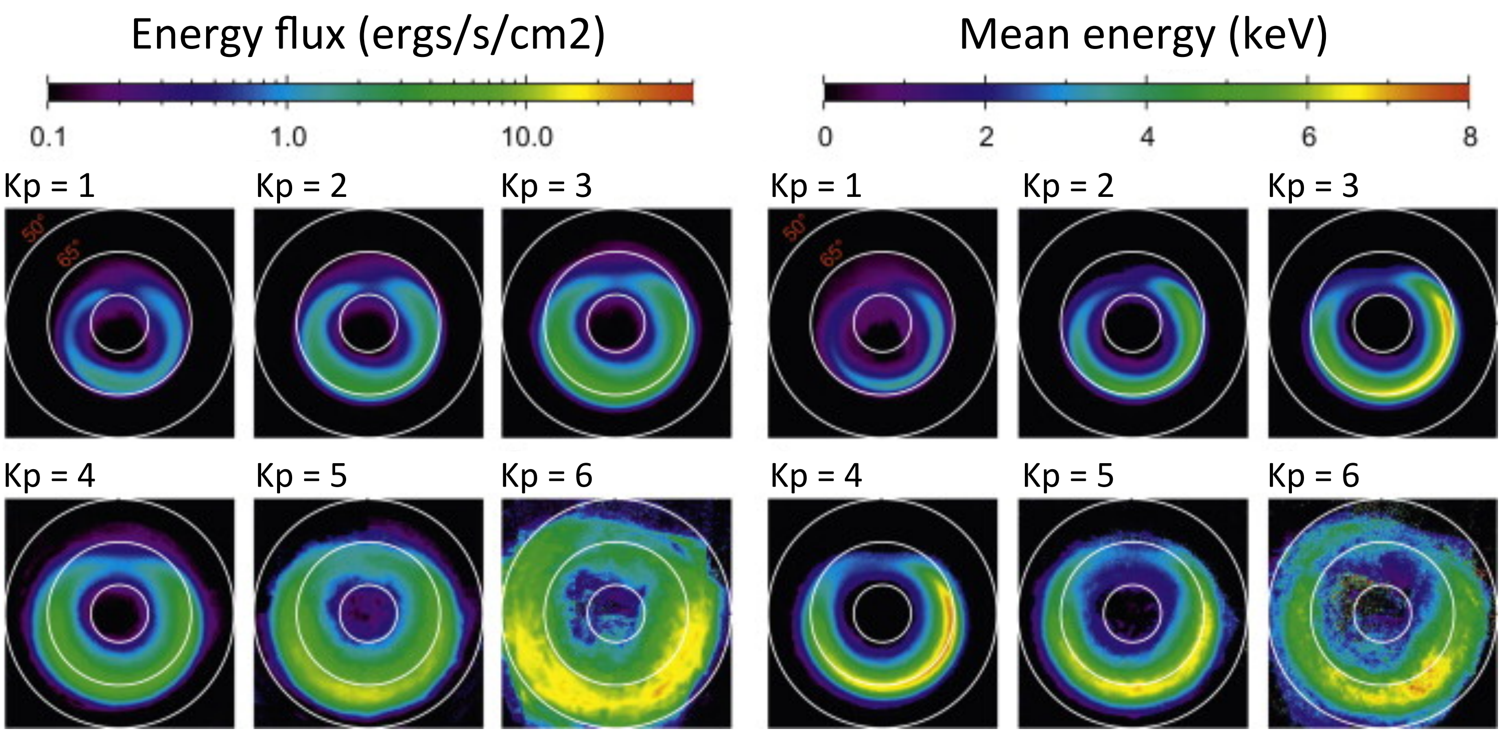

Zhang and Paxton, [2008]

Emission data

Reconstruction of conductances from combination of auroral model and emission data (consecutive DE-1 passes)

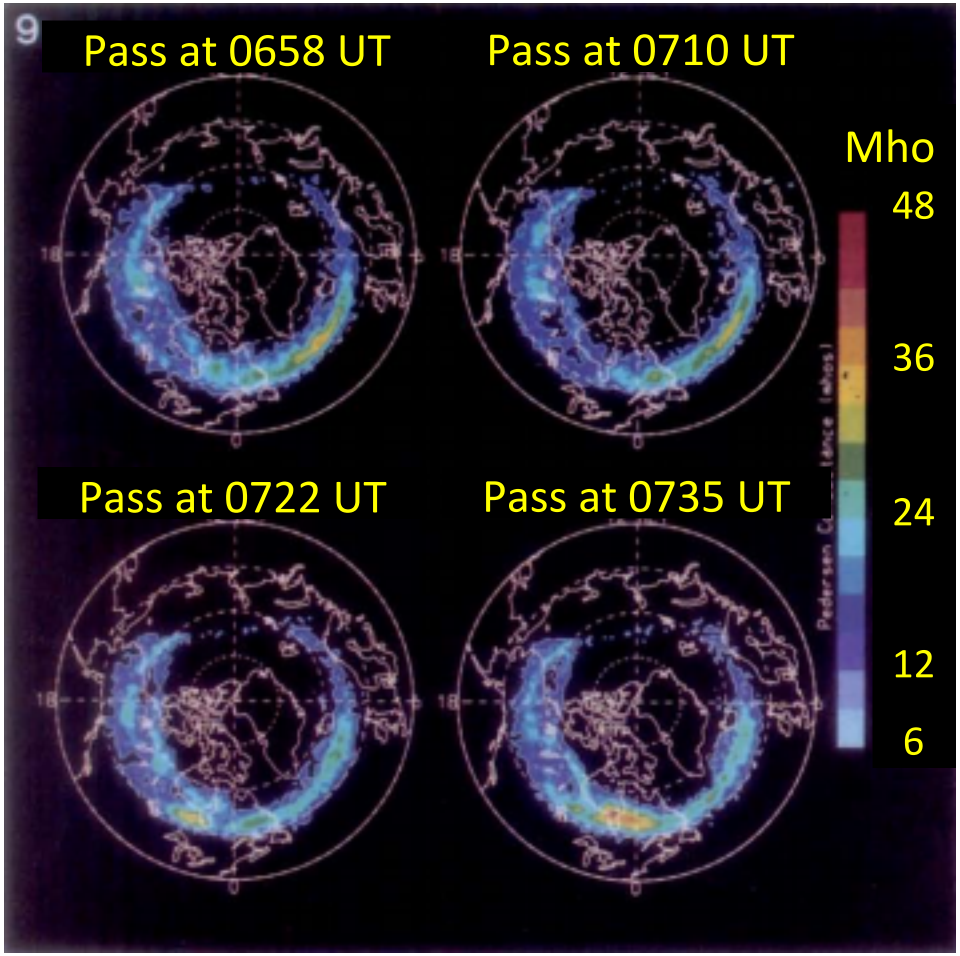

Lummerzheim et al., [1991]

Maxwellian precipitation assumption

Emission data

Reconstruction of conductances from combination of auroral model and emission data (consecutive DE-1 passes)

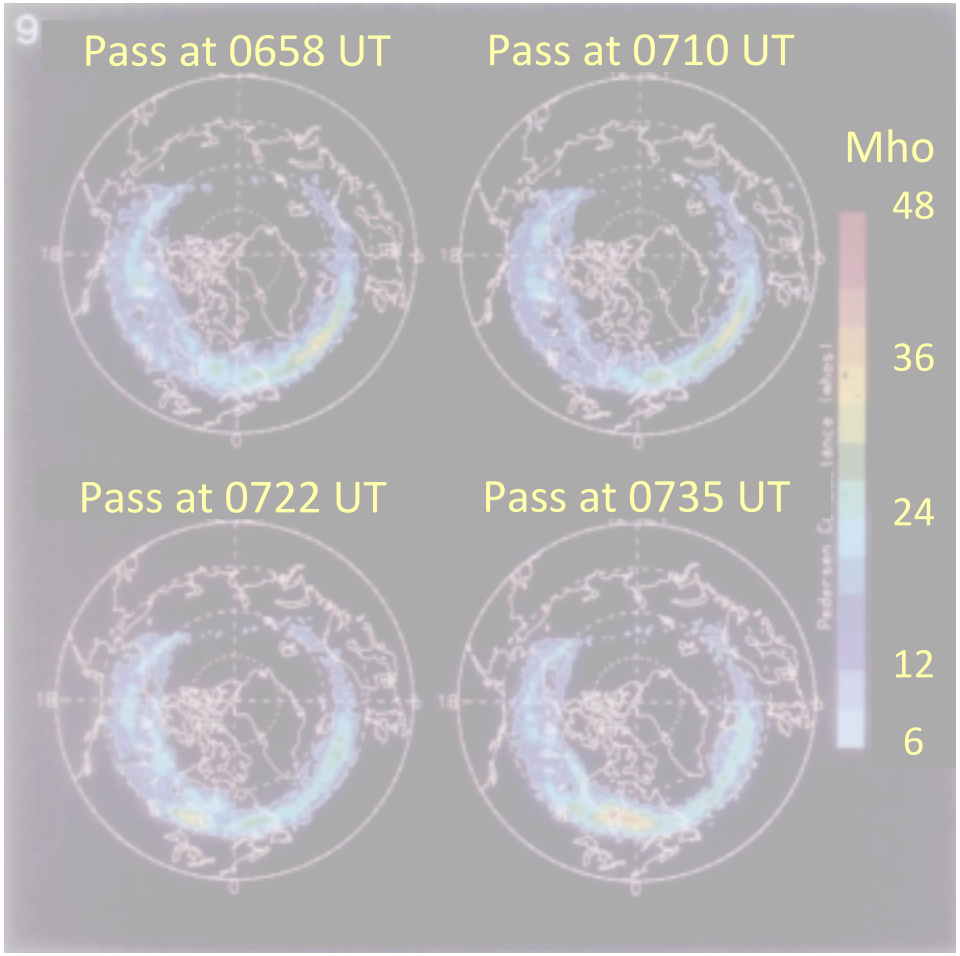

Lummerzheim et al., [1991]

Maxwellian precipitation assumption

Many similar studies:

Germany et al., [1994]
Aksnes et al., [2002]
Coumans et al., [2004]

Reconstruction of conductances from combination of auroral model and emission data (consecutive DE-1 passes)

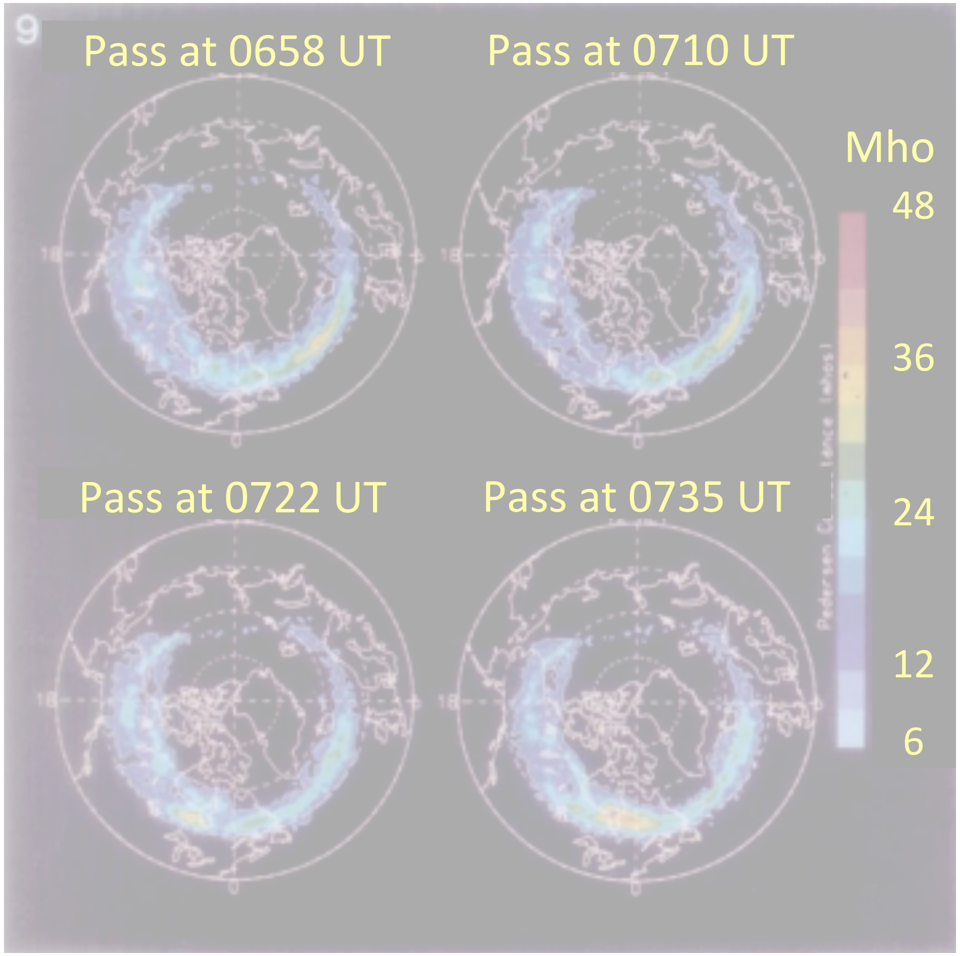

Lummerzheim et al., [1991]

Maxwellian precipitation assumption

Many similar studies:

Germany et al., [1994]
Aksnes et al., [2002]
Coumans et al., [2004]

Substorm modeling:

Gjerloev et al., [2000]
Aksnes et al., [2002]
Coumans et al., [2004]

Magnetometer data

Ground-based

Ahn et al., [1983, 1998]

Space-based (by ensuring consistency with FACs)

Marsal et al., [2015]

Magnetometer data: Ground-based

Empirical relationships between ground magnetometer perturbations and ISR-derived conductances developed and full distributions created

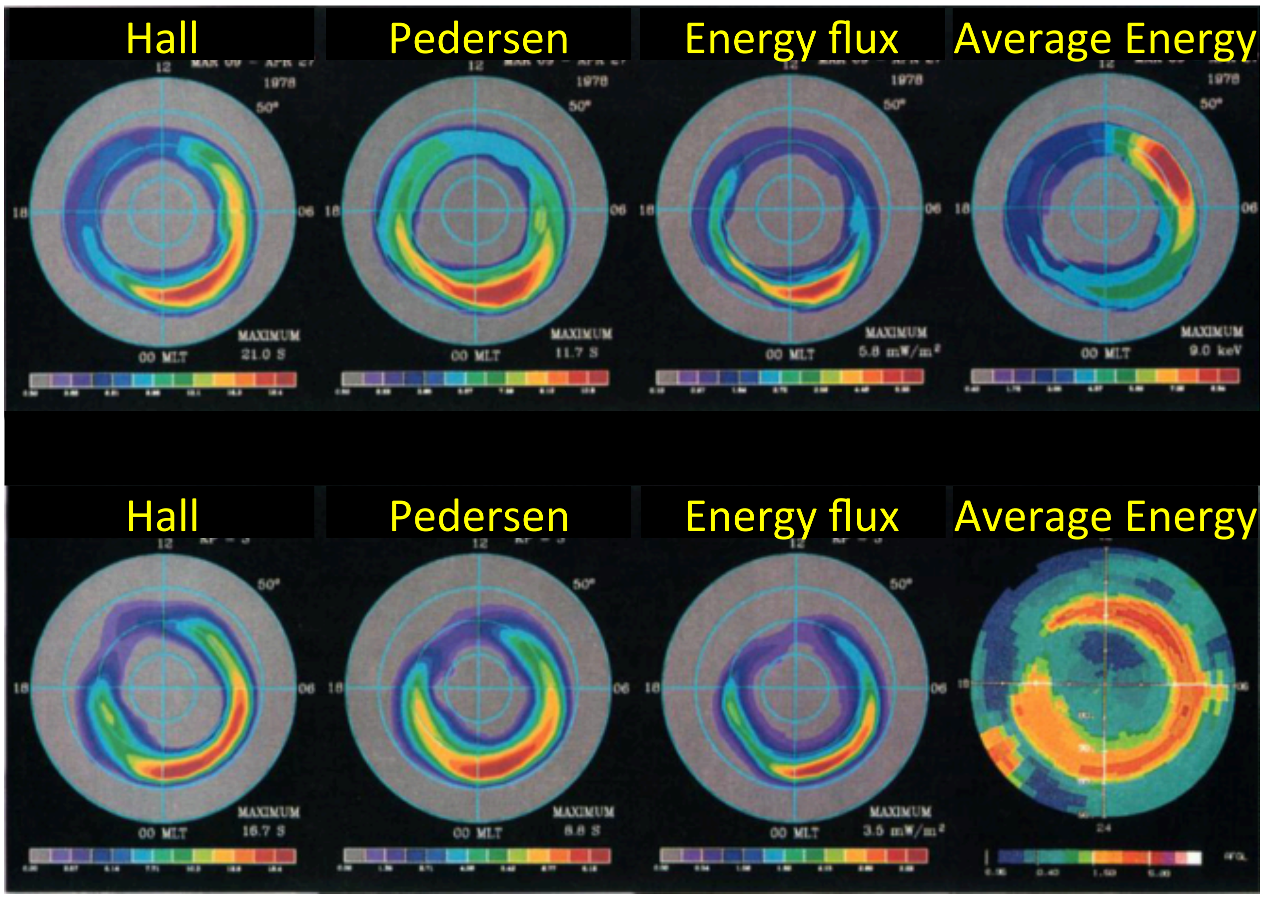

Ahn model

Hardy model

Ahn et al., [1998]

Magnetometer data: Space-based

TIE-GCM conductivities made consistent with FACs derived from AMPERE magnetic perturbations show effects of discrete precipitation

AMPERE FACs

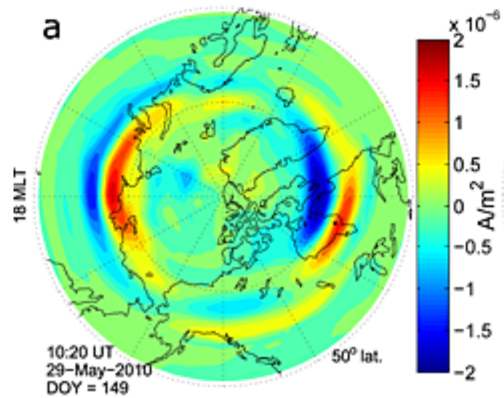

Maxwellian precipitation assumption

TIE-GCM Hall conductance

TIE-GCM Hall conductance consistent with AMPERE FACs

Marklund et al., [1988] model Hall conductance

Marsal, [2015]

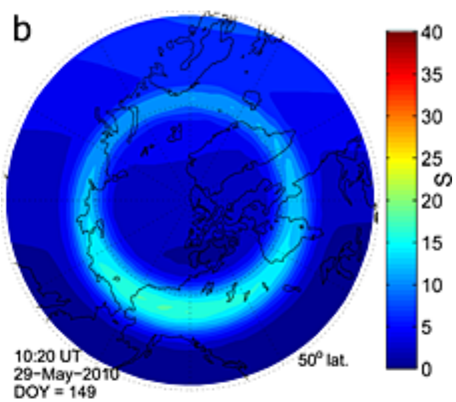

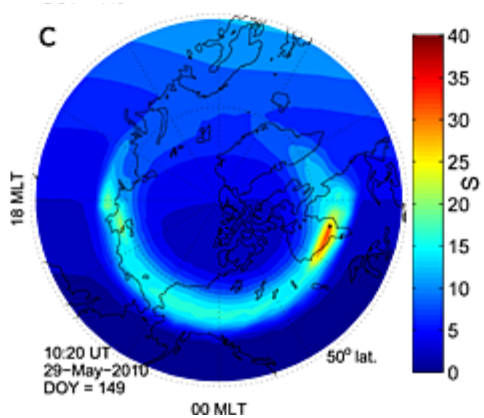

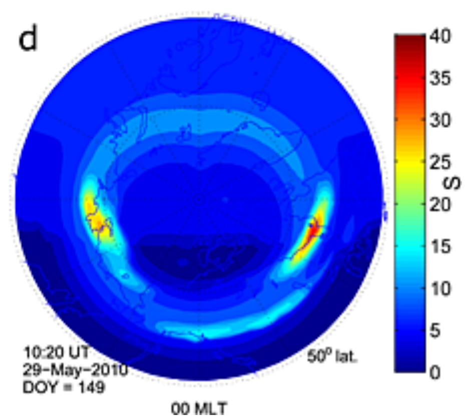

Multiple data sources

Data combined to estimate height-integrated conductances

AMPERE, DMSP, Oersted magnetometers
Ground magnetometers
} $\mathbf{J}_\perp$

DMSP ion drift
SuperDARN plasma convection
} $\mathbf{E}_\perp$

$$\Sigma_H = \frac{\hat{\mathbf{r}} \cdot (\mathbf{J}_\perp \times \mathbf{E}_\perp)}{|\mathbf{E}_\perp|^2}$$

$$\Sigma_P = \frac{\mathbf{J}_\perp \cdot \mathbf{E}_\perp}{|\mathbf{E}_\perp|^2}$$

Amm et al., [2001]

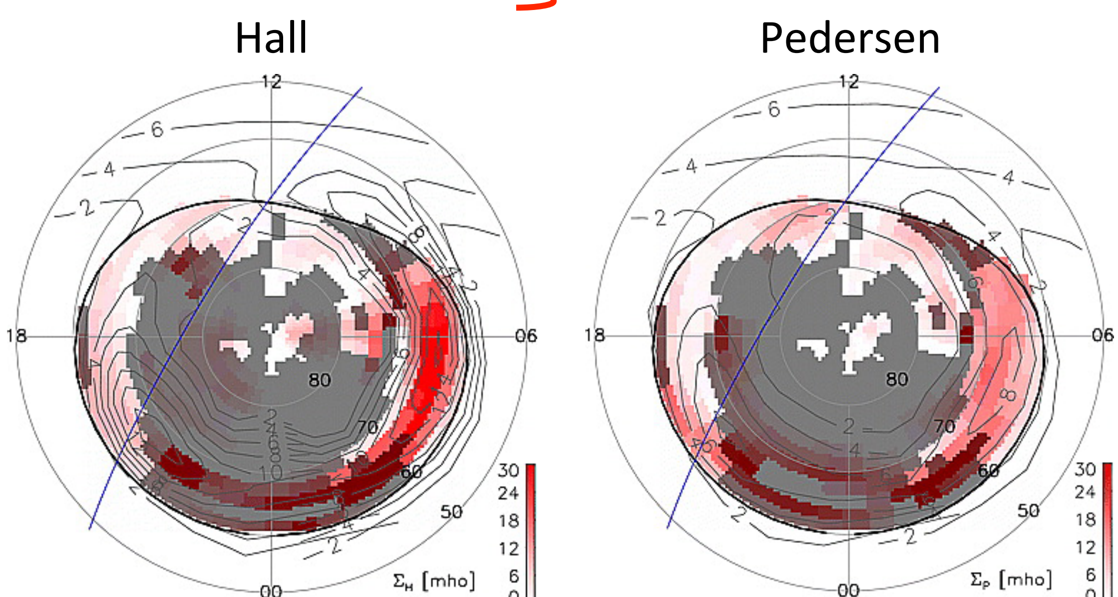

Green et al., [2007]

What's next?

What's next?

Past modeling:

Particle precipitation spectra assumption

2D only

Empirical modeling

Generally limited to single data source -> different approaches paint different picture

What's next?

~~Past modeling:~~
What is needed?

Remove ~~Particle precipitation spectra assumption~~ Particle precipitation spectra assumption

3D ~~2D only~~

Focus on modeling small scales in global analyses ~~empirical modeling~~

Remove limitation ~~Generally limited~~ to single data source -> create consistent ~~different approaches paint different~~ picture

New approach: Optimal interpolation method

Optimally combine information from **observations** and a **background model**, taking into account **error properties** of both

Visually:

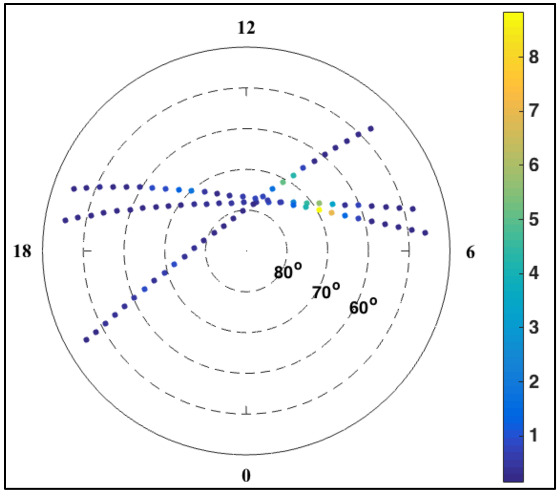

Observations

Minimize observation-model difference in least squares sense

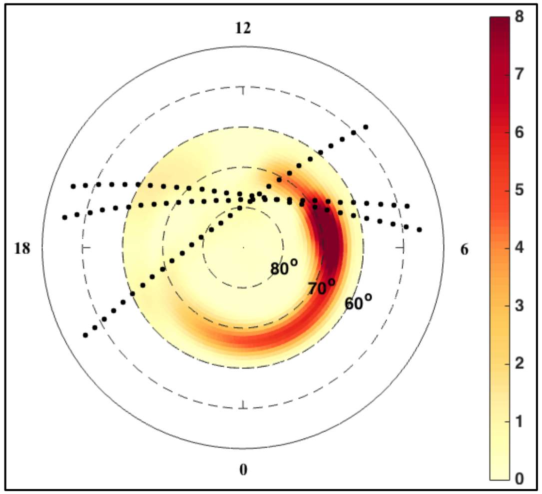

Analysis field

McGranaghan et al., [2015a, b; 2016a, b (in. prep)]

New approach: Optimal interpolation method

Optimally combine information from **observations** and a **background model**, taking into account **error properties** of both

See poster tonight:

DATA-04 Reconstruction of three-dimensional auroral ionospheric conductivities via an assimilative technique

Visually:

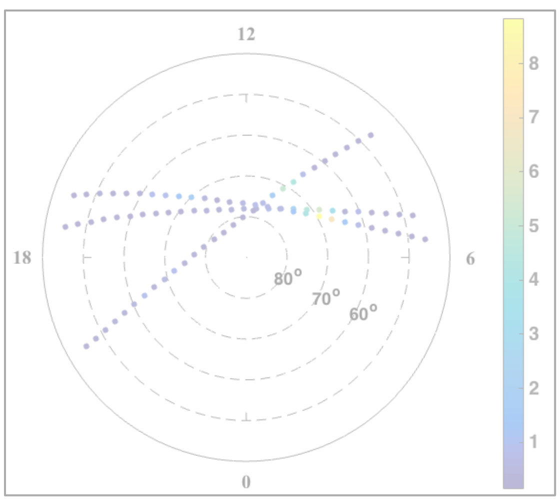

Observations

M
model difference in least squares sense

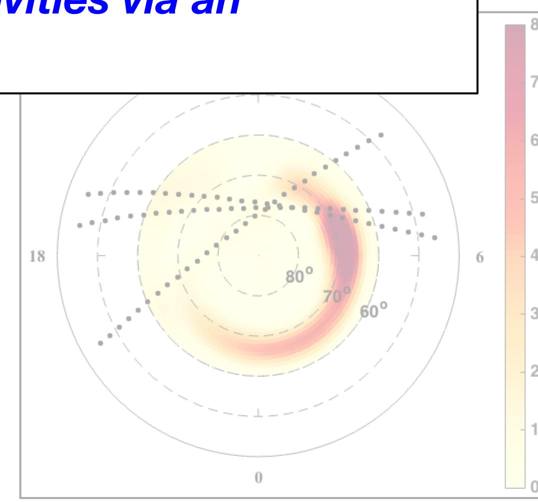

Analysis field

McGranaghan et al., [2015a, b; 2016a, b (in. prep)]

Many different approaches to conductivity/conductance modeling

- Consistencies and disagreement

Fragmented understanding needs to be unified

New assimilative approach can bring together diverse data

- Yields estimates of uncertainty
- More difficult to use than empirical models
- How to use with magnetospheric models?

References

Ahn, B.-H., A. D. Richmond, Y. Kamide, H. W. Kroehl, B. A. Emery, O. de la Beaujardiere, and S.-I. Akasofu (1998), An ionospheric conductance model based on ground magnetic disturbance data, Journal of Geophysical Research: Space Physics, 103 (A7), 14,769-14,780, doi: 10.1029/97JA03088.

Aksnes, A., J. Stadsnes, J. Bjordal, N. stgaard, R. R. Vondrak, D. L. Detrick, T. J. Rosenberg, G. A. Germany, and D. Chenette (2002), Instantaneous ionospheric global conductance maps during an isolated substorm, Annales Geophysicae, 20 (8), 1181-1191, doi:10.5194/angeo-20-1181-2002.

Amm, O. (2001), The elementary current method for calculating ionospheric current systems from multisatellite and ground magnetometer data, J. Geophys. Res., 106(A11), 24,843 – 24,856.

Amm, O., A. Aruliah, S. C. Buchert, R. Fujii, J. W. Gjerloev, A. Ieda, T. Matsuo, C. Stolle, H. Vanhamaki, and A. Yoshikawa (2008), Towards understanding the electrodynamics of the 3-dimensional high-latitude ionosphere: Present and future, Annales Geophysicae, 26 (12), 3913-3932, doi:10.5194/angeo-26-3913-2008.

Coumans, V., J.-C. Gerard, B. Hubert, M. Meurant, and S. B. Mende (2004), Global auroral conductance distribution due to electron and proton precipitation from IMAGE-FUV observations, Annales Geophysicae, 22 (5), 1595-1611, doi:10.5194/angeo-22-1595-2004.

Dimant, Y. S., and M. M. Oppenheim (2011), Magnetosphere-ionosphere coupling through *E* region turbulence: 2. Anomalous conductivities and frictional heating, J. Geophys. Res., 116, A09304, doi:10.1029/2011JA016649.

Germany, G. A., D. G. Torr, P. G. Richards, M. R. Torr, and S. John (1994), Determination of ionospheric conductivities from FUV auroral emissions, Journal of Geophysical Research: Space Physics, 99 (A12), 23,297-23,305, doi:10.1029/94JA02038.

Germany, G. A., G. K. Parks, M. Brittnacher, J. Cumnock, D. Lummerzheim, J. F. Spann, L. Chen, P. G. Richards, and F. J. Rich (1997), Remote determination of auroral energy characteristics during substorm activity, Geophysical Research Letters, 24 (8), 995-998, doi: 0.1029/97GL00864.

References

Gjerloev, J. W., and R. A. Homan (2000), Height-integrated conductivity in auroral substorms: 2. Modeling, Journal of Geophysical Research: Space Physics, 105 (A1), 227-235, doi: 10.1029/1999JA900353.

Green, D. L., C. L. Waters, H. Korth, B. J. Anderson, A. J. Ridley, and R. J. Barnes (2007), Technique: Large-scale ionospheric conductance estimated from combined satellite and ground-based electromagnetic data, J. Geophys. Res., 112, A05303, doi: 10.1029/2006JA012069.

Hardy, D. A., M. S. Gussenhoven, and E. Holeman (1985), A statistical model of auroral electron precipitation, Journal of Geophysical Research: Space Physics, 90 (A5), 4229-4248, doi: 10.1029/JA090iA05p04229.

Hardy, D. A., M. S. Gussenhoven, R. Raistrick, and W. J. McNeil (1987), Statistical and functional representations of the pattern of auroral energy flux, number flux, and conductivity, Journal of Geophysical Research: Space Physics, 92 (A11), 12,275-12,294, doi:10.1029/JA092iA11p12275.

Hardy, D. A., M. S. Gussenhoven, and D. Brautigam (1989), A statistical model of auroral ion precipitation, Journal of Geophysical Research: Space Physics, 94 (A1), 370-392, doi: 10.1029/JA094iA01p00370.

Fuller-Rowell, T. J., and D. S. Evans (1987), Height-integrated Pedersen and Hall conductivity patterns inferred from the TIROS-NOAA satellite data, Journal of Geophysical Research: Space Physics, 92 (A7), 7606-7618, doi:10.1029/JA092iA07p07606.

Galand, M., and A. D. Richmond (2001), Ionospheric electrical conductances produced by auroral proton precipitation, Journal of Geophysical Research: Space Physics, 106 (A1), 117-125, doi: 10.1029/1999JA002001.

Lotko, W., R. H. Smith, B. Zhang, J. E. Ouellette, O. J. Brambles, and J. G. Lyon (2014), Ionospheric control of magnetotail reconnection, Science, 345 (6193), 184-187, doi: 10.1126/science.1252907.

Lummerzheim, D., M. Rees, J. Craven, and L. Frank (1991), Ionospheric conductances derived from DE-1 auroral images, Journal of Atmospheric and Terrestrial Physics, 53 (34), 281-292, doi:http://dx.doi.org/10.1016/0021-9169(91)90112-K, ionospheric Signatures of Magnetospheric Phenomena.

References

Marklund, G. T., L. G. Blomberg, K. Stasiewicz, J. S. Murphree, R. Pottelette, L. J. Zanetti, T. A. Potemra, D. A. Hardy, and F. J. Rich (1988), Snapshots of high-latitude electrodynamics using Viking and DMSP F7 observations, Journal of Geophysical Research: Space Physics, 93 (A12), 14,479-14,492, doi:10.1029/JA093iA12p14479.

Marsal, S. (2015), Conductivities consistent with Birkeland currents in the AMPERE-driven TIE-GCM, Journal of Geophysical Research: Space Physics, 2015JA021385, doi: 10.1002/2015JA021385.

McGranaghan, R., D. J. Knipp, S. C. Solomon, and X. Fang (2015a), A fast, parameterized model of upper atmospheric ionization rates, chemistry, and conductivity, Journal of Geophysical Research: Space Physics, 2015JA021146, doi: 10.1002/2015JA021146.

McGranaghan, R., D. J. Knipp, T. Matsuo, H. Godinez, R. J. Redmon, S. C. Solomon, and S. K. Morley (2015b), Modes of high-latitude auroral conductance variability derived from DMSP energetic electron precipitation observations: Empirical orthogonal function analysis, Journal of Geophysical Research: Space Physics, 2015JA021828, doi:10.1002/2015JA021828.

McGranaghan, R., D. J. Knipp, T. Matsuo, and E. Cousins (2016), Optimal interpolation analysis of high-latitude ionospheric Hall and Pedersen conductivities: Application to assimilative ionospheric electrodynamics reconstruction, J. Geophys. Res. Space Physics, 121, 4898–4923, doi:10.1002/2016JA022486.

Pulkkinen, A., E. Bernabeu, J. Eichner, A. Viljanen, and C. Ngwira (2015), Regional-scale high-latitude extreme geoelectric fields pertaining to geomagnetically induced currents, Earth, Planets and Space, 67(1), 93, doi:10.1186/s40623-015-0255-6.

Raeder, J., R. L. McPherron, L. A. Frank, S. Kokubun, G. Lu, T. Mukai, W. R. Paterson, J. B. Sigwarth, H. J. Singer, and J. A. Slavin (2001), Global simulation of the Geospace Environment Modeling substorm challenge event, Journal of Geophysical Research: Space Physics, 106 (A1), 381-395, doi:10.1029/2000JA000605.

References

Richmond, A. D., and Y. Kamide (1988), Mapping electrodynamic features of the high-latitude ionosphere from localized observations: Technique, Journal of Geophysical Research: Space Physics, 93 (A6), 5741-5759, doi:10.1029/JA093iA06p05741.

Richmond, A. D., and J. P. Thayer (2000), Ionospheric electrodynamics: A tutorial, in Magnetospheric Current Systems, edited by S.-I. Ohtani, R. Fujii, M. Hesse, and R. L. Lysak, pp. 131-146, American Geophysical Union, Washington, D. C., doi:10.1029/GM118p0131.

Ridley, A. J., T. I. Gombosi, and D. L. DeZeeuw (2004), Ionospheric control of the Magnetosphere: Conductance, Annales Geophysicae, 22 (2), 567-584, doi:10.5194/angeo-22-567-2004.

Robinson, R. M., R. R. Vondrak, K. Miller, T. Dabbs, and D. Hardy (1987), On calculating ionospheric conductances from the fux and energy of precipitating electrons, Journal of Geophysical Research: Space Physics, 92 (A3), 2565-2569, doi:10.1029/JA092iA03p02565.

Spiro, R. W., P. H. Rei, and L. J. Maher (1982), Precipitating electron energy flux and auroral
zone conductances-an empirical model, Journal of Geophysical Research: Space Physics, 87 (A10), 8215-8227, doi:10.1029/JA087iA10p08215.

Winglee, R. M., V. O. Papitashvili, and D. R. Weimer, Comparison of the high-latitude ionospheric electrodynamics inferred from global simulations and semi-empirical models for the January 1992 GEM campaign, J. Geophys. Res., 102, 26,961, 1997.

Zhang, Y., and L. Paxton (2008), An empirical Kp-dependent global auroral model based on TIMED/GUVI FUV data, Journal of Atmospheric and Solar-Terrestrial Physics, 70 (89), 1231-1242, doi:http://dx.doi.org/10.1016/j.jastp.2008.03.008.

Backup slides

Specialized modeling

Regional

Amm et al., [2015] – Swarm-based estimates

Auroral substorms

Germany et al., [1997]

Gjerloev et al., [2000]

Turbulent conductivities

Dimant and Oppenheim, [2011]

Better organization of conductance features

Using dynamic auroral boundary coordinates? (to my knowledge this has not been done)

Challenges

Issues with AMIE and MHD models likely traced to conductivity specification

- *Winglee et al.*, [1997] – AMIE
- *Raeder et al.*, [2001] – Modeling challenge study
- *Pulkkinen et al.*, [2013] – Performance of various MHD models

Time resolution of methods

- Substorm dynamics require much finer resolution
- *Gjerloev.*, [2000] – emission data can produce conductances at time resolution of measurement

Three-dimensional modeling

- *Amm et al.*, [2008] – importance of 3D ionospheric specification

Multi-scale understanding

How does this impact magnetospheric modeling?

Where/how to place conductances?

Ridley et al., [2004]

Lotko et al., [2014]

1. Determine FACs at inner boundary (~3.5 R_E, generally)
2. Map FACs from inner boundary to ionosphere (using background magnetic field)
3. Generate a conductance pattern

   ➔How?
4. Map ionospheric potential to inner boundary
5. Solve electric fields and velocity fields at inner boundary and use in MHD model

How does this impact magnetospheric modeling?

Where/how to place conductances?

Ridley et al., [2004]

Lotko et al., [2014]

1. Determine FACs at inner boundary (~3.5 R_E, generally)
2. Map FACs from inner boundary to ionosphere (using background magnetic field)
3. Generate a conductance pattern

   ➔How?
4. Map ionospheric potential to inner boundary
5. Solve electric fields and velocity fields at inner boundary and use in MHD model

Ways MHD codes solve conductance:

Simple

- Assume uniform *Fedder and Lyon*, [1987]
- Precipitation relationships
  a. Diffuse = f(plasma sheet T)
  b. Discrete = *Knight* (1972)
- Empirically from FACs *Ridley et al.*, [2004]
- Causal electron precipitation *Zhang et al.*, [2015]
- Introduce conductance distributions

Complex

So, where are we?

Dan Weimer at *Unsolved Problems in Magnetospheric Physics* conference:

> 'What is needed within the community is a comprehensive conductivity model, with software code provided. Needs to use IMF values, not just Kp. It likely would be better to use EUV indices, rather than $F_{10.7}$'

Other perspectives…

New approach: Optimal interpolation method

- Optimally combine information from **observations** and a **background model**, taking into account **error properties** of both

$$\vec{x}_a = \vec{x}_b + K\left(\vec{y} - H\vec{x}_b\right)$$

$$K = P_b H^{\mathrm{T}}\left(H P_b H^{\mathrm{T}} + R\right)$$

$\vec{x}_a$ – Analysis field

$\vec{x}_b$ – Background model

K – Kalman gain

$\vec{y}$ – Observations

H – Forward operator

P_b – Background model error covariance

R – Observational error covariance

New approach: Assimilation

Objective analysis and empirical orthogonal functions allow:

- Estimates of conductivity in 3D, without assumption of particle precipitation spectrum
- Facilitate bringing together growing, diverse data
- Provides estimate of uncertainty in solution

- More complex than empirical models
- Not capable of forecasting, currently
- How to bring into magnetospheric models?

Conductance control of magnetosphere

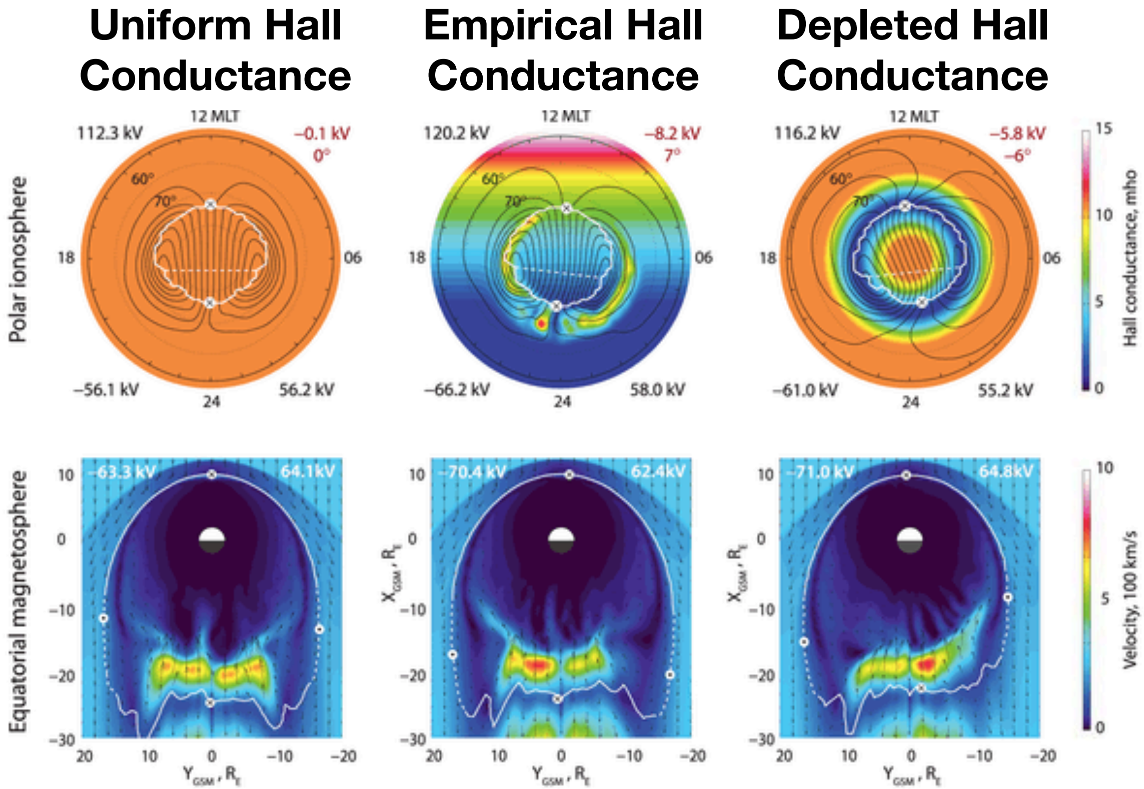

Fig. 3. Effect of ionospheric Hall conduction on convection in the ionosphere and plasmasheet. Top: Simulated ionospheric convection (8 kV contours) and Hall conductance distributions (color). The distribution of Pedersen conductance is a uniform 5 S for the simulations in the left and right panels and is similar to the Hall distribution in the causal conductance case but smaller in magnitude. Total cross polar cap potential is given in the upper left of each panel. The dusk minimum and dawn maximum are given below each panel. The white contour is the x-line mapped along magnetic field lines from the magnetosphere. The circled cross locates its intersection with the zero-potential contour. Bottom: Simulated equatorial magnetosphere with velocity vectors overlaid on velocity magnitude in color. $B_z = 0$ contour (magnetic x-line) is shown in white. Minimum and maximum reconnection potentials from Fig. 4 occur at circled dots, with location uncertainty confined to the dashed segments where the reconnection rate is nearly zero. The circled cross is the field-line mapping of the corresponding point in the ionosphere.

Lotko et al. [2014]

Electrons → Substorm Conductance

Fundamentals - **Current Understanding/Modeling** - What's next?

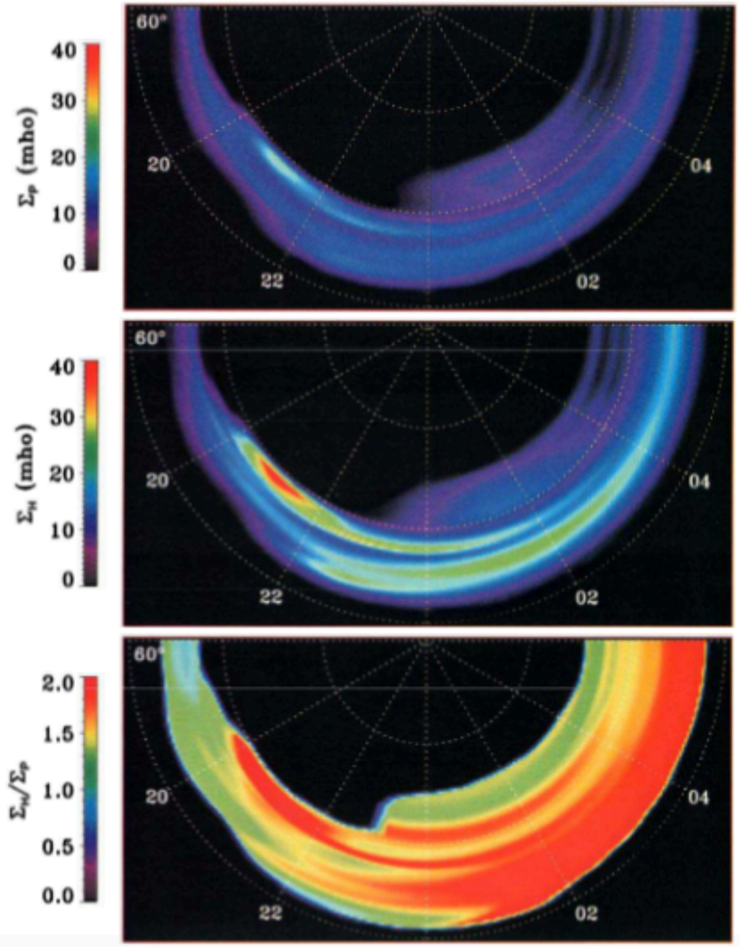

Plate 1. Polar plots showing the Pedersen conductance, the Hall conductance, and the Hall to Pedersen ratio as function of invariant latitude and a generalized magnetic local time derived from the average passes shown in Figure 1.

Text here

Functional spectral precipitation assumption?

Gjerloev and Hoffman, [2000]

Combination of auroral and solar contributions

$$\sigma^2_{\mathrm{total}} = \sigma^2_{\mathrm{auroral}} + \sigma^2_{\mathrm{solar}}$$ Correct

These operations do not commute

$$\Sigma^2_{\mathrm{total}} = \Sigma^2_{\mathrm{auroral}} + \Sigma^2_{\mathrm{solar}}$$ Introduces error

Magnetometer data: Space-based Marklund et al., [1988] model

$$\Sigma^2_{P_{\text{total}}} = \Sigma^2_{P_0} + \Sigma^2_{P_g} + \Sigma^2_{P_{UV}} + \Sigma^2_{P_{j_{||}}}$$

$$\Sigma^2_{H_{\text{total}}} = \Sigma^2_{H_0} + \Sigma^2_{H_g} + \Sigma^2_{H_{UV}} + \Sigma^2_{H_{j_{||}}}$$

- $\Sigma^2_{H_0}$: Background component
- $\Sigma^2_{H_g}$: Avg. auroral zone component
- $\Sigma^2_{H_{UV}}$: Solar EUV component
- $\Sigma^2_{H_{j_{||}}}$: Upward FAC enhanced component

Multiple data sources

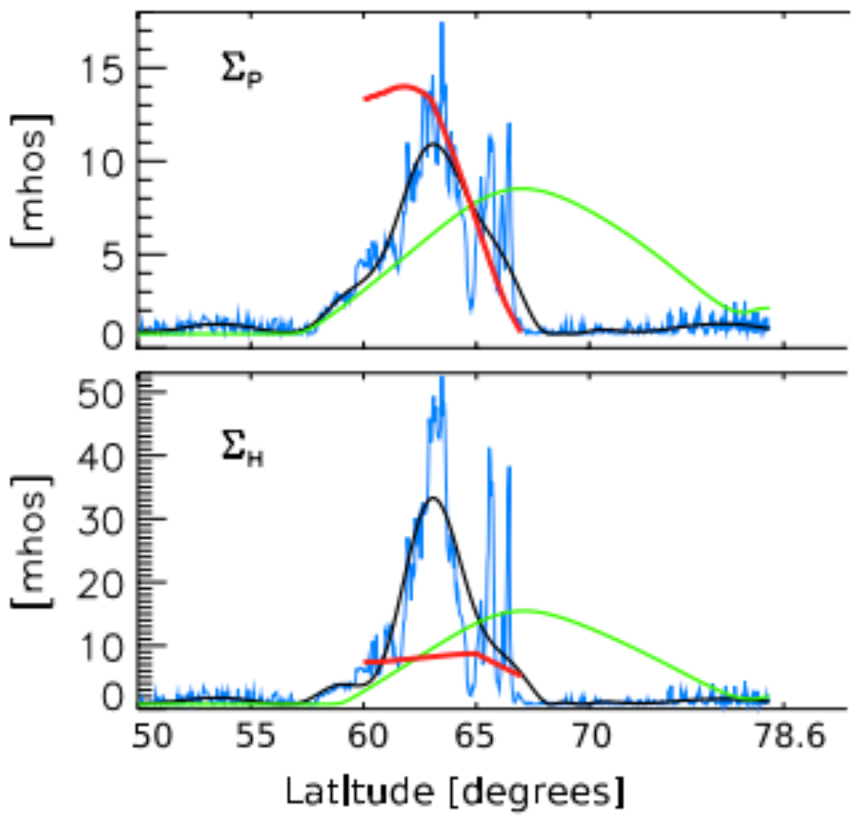

Figure 13. Conductance data along the F15 DMSP track (2100 to 1100 MLT, cf., Figures 9 and 10; 0251:0422 UT). Σ^{DMSP} (raw: blue; filtered: black), conductance model (green) and calculated from electromagnetic data (red).

Green et al., [2007]

$$\Sigma_H = \frac{\hat{\mathbf{r}} \cdot (\mathbf{J}_\perp \times \mathbf{E}_\perp)}{|\mathbf{E}_\perp|^2}$$

$$\Sigma_P = \frac{\mathbf{J}_\perp \cdot \mathbf{E}_\perp}{|\mathbf{E}_\perp|^2}$$

Amm et al., [2001]

Ionospheric Conductivity

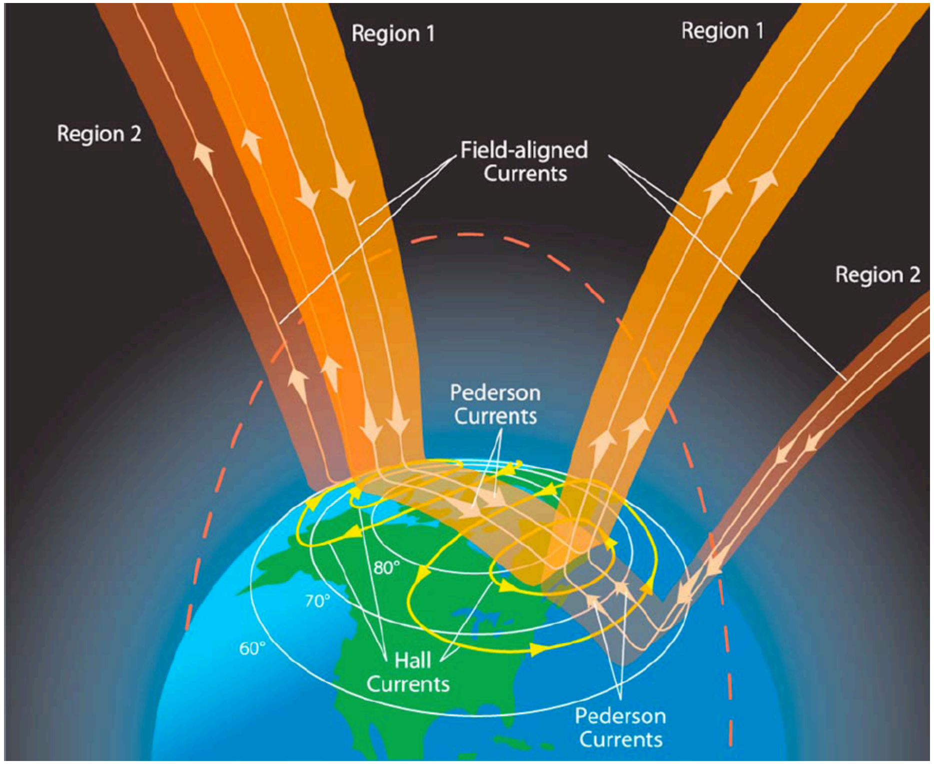

$$\mathbf{J} = \tilde{\sigma} \cdot \mathbf{E}$$

$$= \sigma_P \mathbf{E}_\perp + \sigma_H \hat{\mathbf{B}} \times \mathbf{E} + \sigma_\parallel \mathbf{E}_\parallel$$

$$\tilde{\sigma} = \begin{bmatrix} \sigma_P & -\sigma_H & 0 \\ \sigma_H & \sigma_P & 0 \\ 0 & 0 & \sigma_\parallel \end{bmatrix}$$

$$\int_h \sigma_x \mathrm{d}h = \Sigma_x$$

Multiple data sources

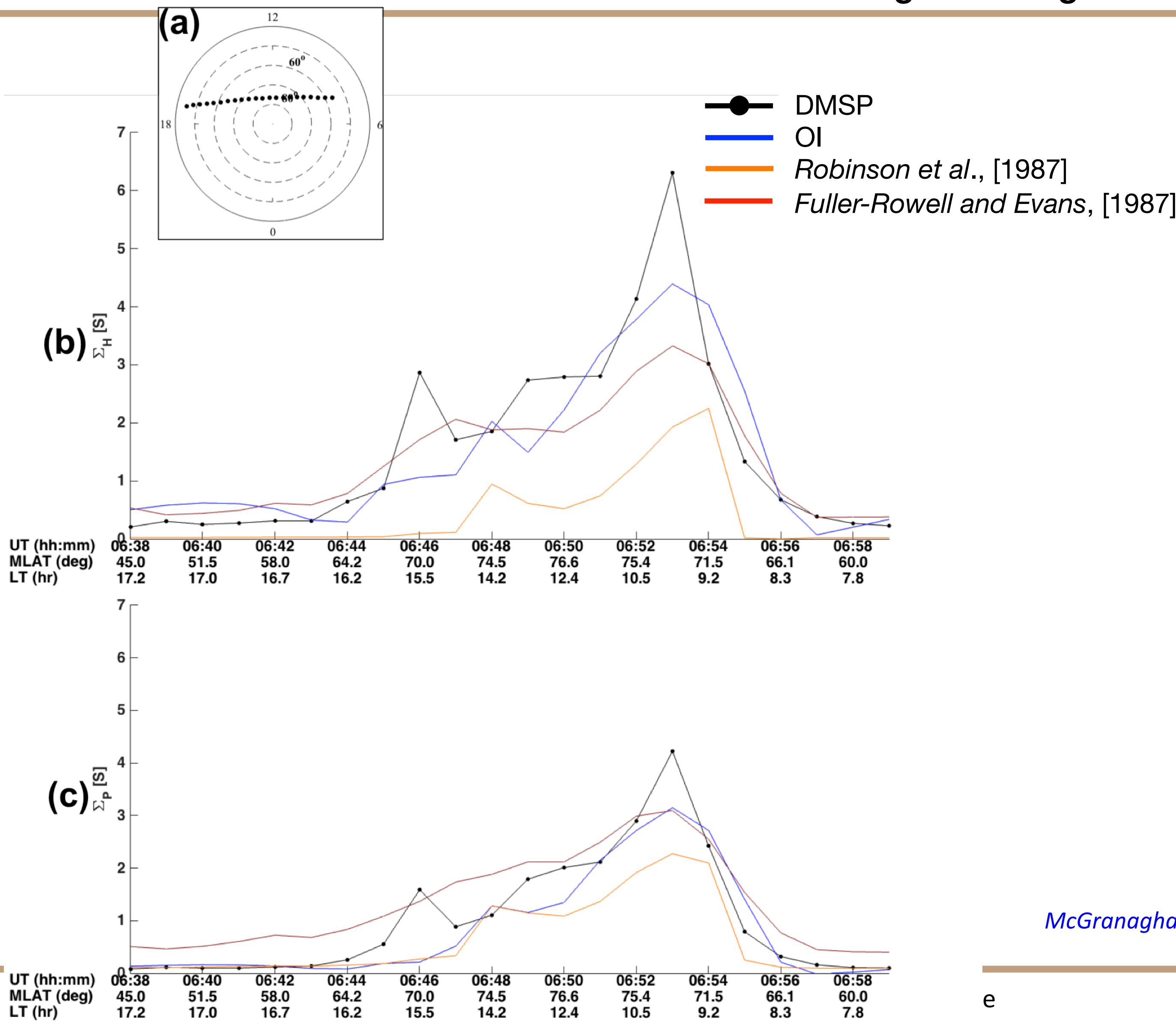

McGranaghan et al., [2016]

New approach: Optimal interpolation method

- Optimally combine information from **observations** and a **background model**, taking into account **error properties** of both
- **Background model**: EOF-based mean
- **Observations**: DMSP particle precipitation data
- **Error properties**:
  - For background model: Estimated from EOFs
  - For DMSP particle precipitation data: Poisson statistics for individual spectra

$$\vec{x}_a = \vec{x}_b + K\left(\vec{y} - H\vec{x}_b\right)$$

$$K = P_b H^{\mathrm{T}}\left(H P_b H^{\mathrm{T}} + R\right)$$

$\vec{x}_a$ – Analysis field

$\vec{x}_b$ – Background model

K – Kalman gain

$\vec{y}$ – Observations

H – Forward operator

P_b – Background model error covariance

R – Observational error covariance

Conductance observation creation:

1. DMSP in-situ electron energy spectrum
2. Conductivity profiles (from GLOW model)
3. Integrate over 80-200 km and apply to all spectra for satellite pass
4. Accumulate over analysis window

Conductance observation creation:

1. DMSP in-situ electron energy spectrum
2. Conductivity profiles (from GLOW model)
3. Integrate over 80-200 km and apply to all spectra for satellite pass
4. Accumulate over analysis window

Obs Creation: [1]Particle Spectrum - [2]Conductivity - [3]Integration - [4]Accumulate

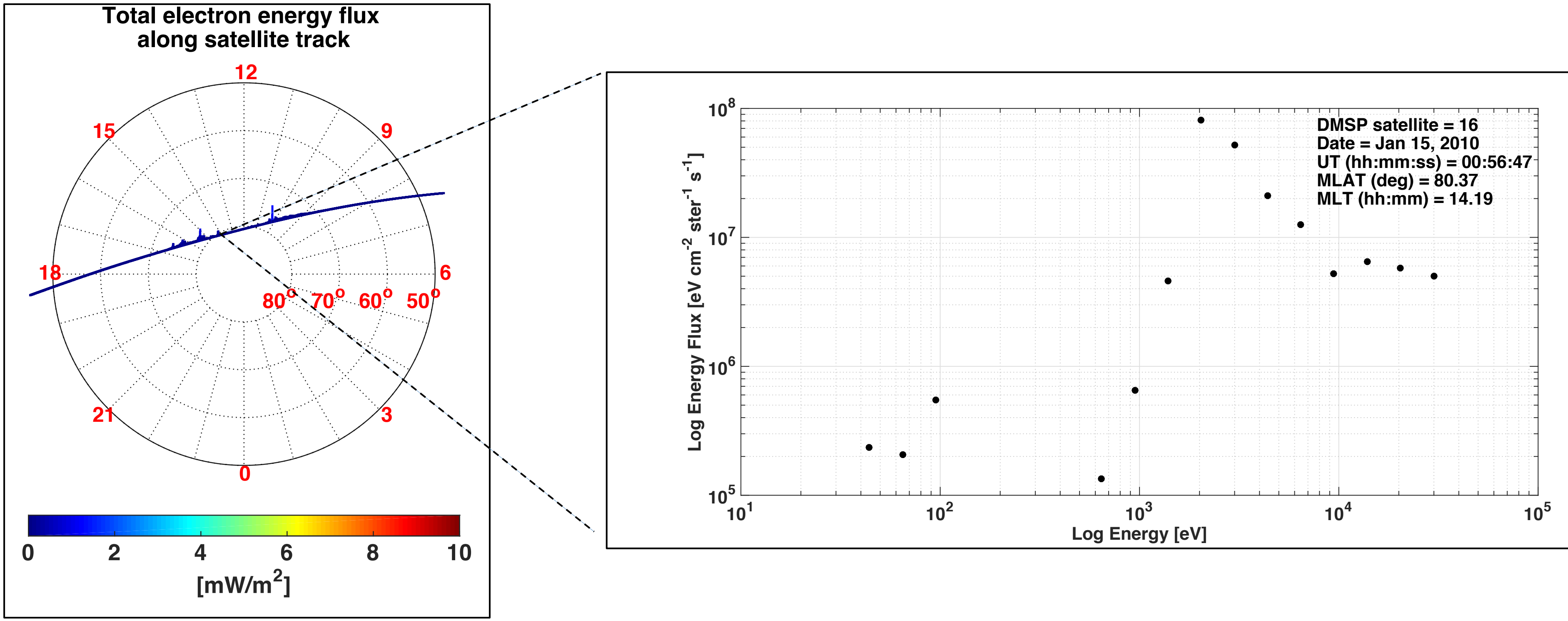

Conductance observation creation:

1. DMSP in-situ electron energy spectrum
2. Conductivity profiles (from GLOW model)
3. Integrate over 80-200 km and apply to all spectra for satellite pass
4. Accumulate over analysis window

Obs Creation: [1]Particle Spectrum - **[2]Conductivity** - [3]Integration - [4]Accumulate

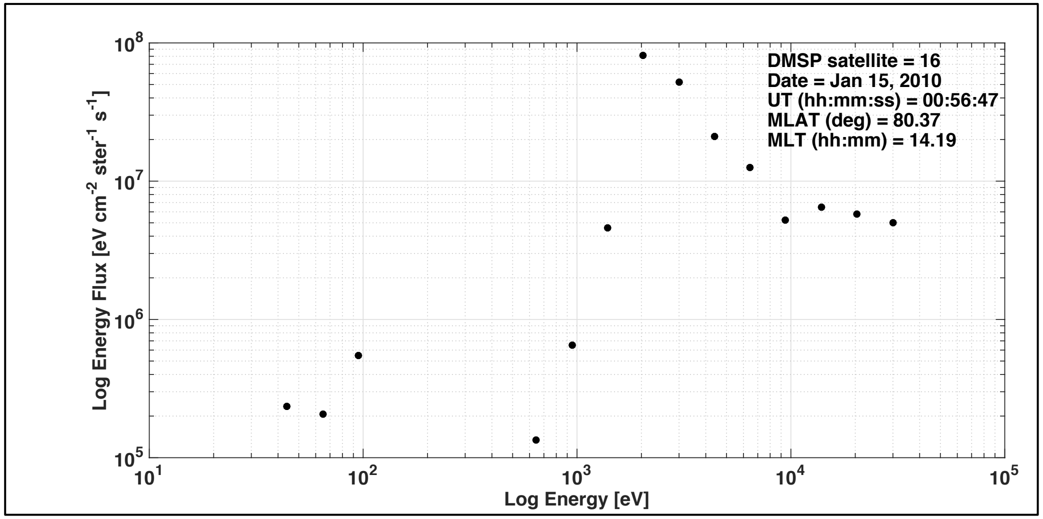

GLOW + conductivity

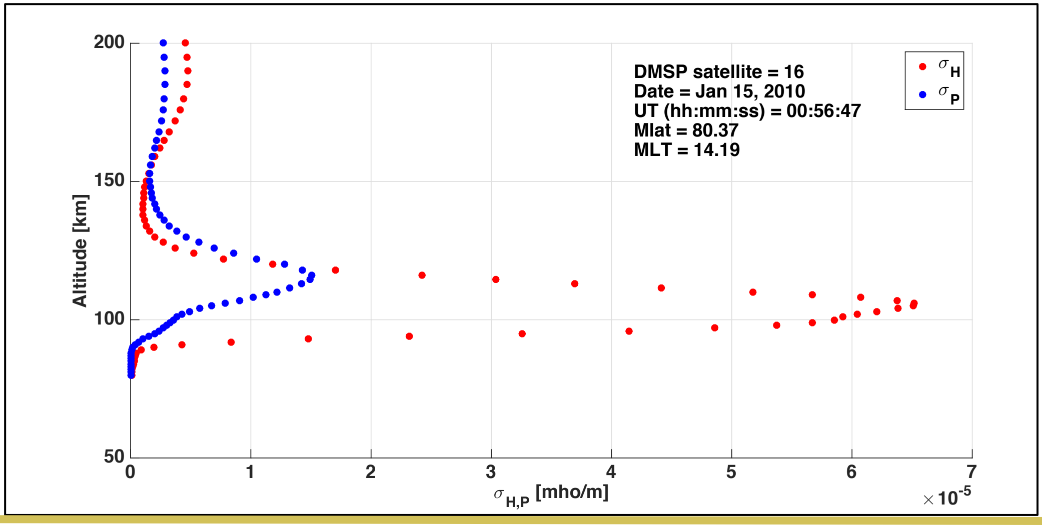

Conductance observation creation:

1. DMSP in-situ electron energy spectrum
2. Conductivity profiles (from GLOW model)
3. Integrate over 80-200 km and apply to all spectra for satellite pass
4. Accumulate over analysis window

Obs Creation: [1]Particle Spectrum - [2]Conductivity - [3]Integration - [4]Accumulate

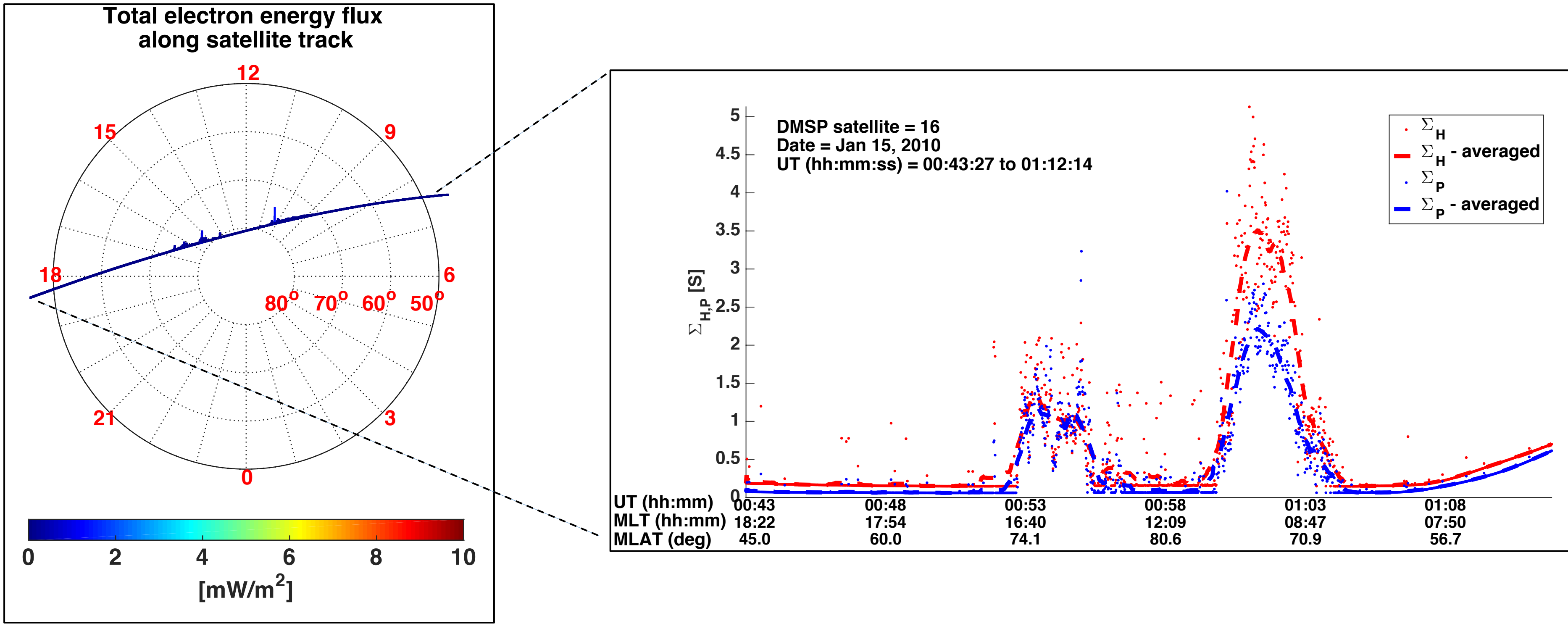

Conductance observation creation:

1. DMSP in-situ electron energy spectrum
2. Conductivity profiles (from GLOW model)
3. Integrate over 80-200 km and apply to all spectra for satellite pass
4. Accumulate over analysis window

Obs Creation: [1]Particle Spectrum - [2]Conductivity - [3]Integration - **[4]Accumulate**

Jan. 15, 2010

UT time (hh:mm:ss) = 00:00:00 to 01:00:00

4. Accumulate over analysis window